

# Mode I Stress Intensity Factors of Sickle-Shaped Surface Cracks in Round Bars

Al Emran Ismail\*

<sup>1</sup>Department of Engineering Mechanics, Faculty of Mechanical and Manufacturing Engineering, Universiti Tun Hussein Onn Malaysia, Batu Pahat, 86400 Johor, MALAYSIA.

Received 01 August 2016; accepted 15 August 2016, available online 15 August 2016

**Abstract:** Nowadays, the sickle-shaped surface crack generally occurred around the bolt under tension due to the stress concentrations occurred at the design discontinuities. The behaviors of these cracks are not really understood and additionally it is hard to find the solutions of stress intensity factors of this kind of cracks. Therefore, the intention of this paper is to present the behavior of these cracks under tension loading. In order to understand the role of these cracks, there are seven crack aspect ratios,  $a/b$  are considered ranging from 0.0 to 1.2. For each crack aspect ratio, there are six relative crack depth,  $a/D$  are used ranging from 0.1 to 0.6. There are two types of loading are used so called free- and fix-stresses. ANSYS finite element program is used to model the crack. Stress intensity factor (SIF) which is based on the J-integral is used to characterize the cracks. For relatively shallow cracks ( $a/D \leq 0.3$ ), the role of SIFs along the crack front is insignificant where the values of SIFs remain flattened along the crack front as  $a/D$  increased. However, for the deeper cracks ( $a/D > 0.3$ ), the effect of  $a/b$  is pronounced on the SIFs. If  $a/b$  is increased from 0.0 to 1.0, higher SIFs are obtained within the central compared with the outer regions. This is due to the fact that the circumferential crack at the both sides of the bar experienced lack of mode I opening mechanism compared with the crack faces of the upper side cracks. It is also found that the SIFs obtained under free tension stress is higher than the SIFs under fix stress due to the fact that free stress condition capable to induce the bending moment effect and therefore widening the crack faces.

**Keywords:** Sickle-Shaped Crack; Surface Cracks; Round Solid Bars; Tension Stress

## 1. Introduction

Round solid bars have many applications in mechanical and structural engineering. They generally used to transmit mechanical power from one location to another points [1]. Some of these bars are exposed to environmental harshness leading to the formation of surface crack [2]. The existence of crack is also due to geometrical discontinuities such notches. Under special circumstances [3], sickle-shaped surface crack occurred around the round bars. There are other types of cracks and the most popular one is semi-elliptical surface crack [3-6]. The review of this crack under tension forces can be found in [7].

Mattheck et al. [8] reported that under certain circumstances, sickle-shaped crack occurred on the surface of solid round bar. They have presented the SIFs for several crack geometries, however they are very limited. Hobbs et al. [9] analyzed experimentally the sickle-shaped cracks in bolts under axial and eccentric loads. It is found that the shape of crack front is insignificantly affected the SIF especially at the middle point along the crack front. However, the shapes of crack fronts have played an important role in varying the SIFs along it. Additionally, the effect of loading eccentricity is found to increase slightly the SIFs at the central point of the crack front.

According to the author's knowledge, the roles of crack geometries on the SIFs are fully discussed. There

are several papers discussed on the SIFs along the crack front of sickle-shaped crack especially when it is subjected to tension forces [10-11]. Carpinteri and Vantadori [10] performed the numerical work on the sickle-shaped surface crack on the round bar under eccentric axial loading. Wide ranges of crack geometries are considered, however the determination of SIFs are limited to the interested locations. Additionally, their work focused more on the analyses of fatigue crack growth of such cracks. In another paper, Carpinteri and Vantadori [11] investigated the behavior of similar crack however they placed the cracks in notches before it is subjected to cyclic tension and bending loading. The effects of stress concentration factor on the SIFs are the main concern.

This paper investigated the stress intensity factors (SIFs) for various geometries of sickle-shaped surface cracks under free- and fix-type tension stresses. There are seven crack aspect ratios,  $a/b$  are used ranging between 0.0 to 1.2. For each  $a/b$ , there are six relative crack depth,  $a/D$  between 0.1 and 0.6. Stress intensity factors based on the J-integral are used to characterize the crack behavior where ANSYS finite element program is used to model the surface cracks.

## 2. Stress Intensity Factor

It is firstly introduced by Rice [13] assuming a crack in two-dimensional plate,  $J$ -integral is defined as a

contour,  $\Gamma$  around the crack tip. It is evaluated counter-clockwise as depicted in Figure 1 and can be expressed as Eq. (1):

$$J = \int_{\Gamma} \left( W dy - \bar{T} \cdot \frac{\partial u}{\partial z} ds \right) \quad (1)$$

where,  $\bar{T}$  is an outward traction vector along the contour,  $\Gamma$  is defined as  $T_i = \sigma_{ij} n_j$  or it is a force per unit length,  $u$  is a displacement vector and  $ds$  is an element on the contour,  $\Gamma$ . While,  $W$  is a strain energy density expressed as Eq. (2):

$$W = \int_0^{\epsilon} \sigma_{ij} d\epsilon_{ij} = \int_0^{\epsilon} \{\sigma\}^T d\{\epsilon\} \quad (2)$$

where,  $\epsilon_{ij}$  is a strain tensor and  $\{\epsilon\}$  represents as a strain vector. In elastic-plastic analysis  $J$ -integral is composed from two parts, elastic  $J$ -integral,  $J_e$  and plastic  $J$ -integral,  $J_p$  as (Kumar et al. [14]) in Eq. (3):

$$J = J_e + J_p \quad (3)$$

where,  $J_e$  can be obtained numerically using finite element analysis (FEA) or by the Eq. (4) (Rahman [15]):

$$J_e = \frac{K_I^2}{\kappa} \quad (4)$$

where,  $K_I$  is the mode I elastic SIF,  $\kappa = E$  for plane stress and  $\kappa = E / (1-\nu^2)$  for plane strain. Since, this work only concerned on the elastic analysis, the plastic term is omitted from Eq. (3).

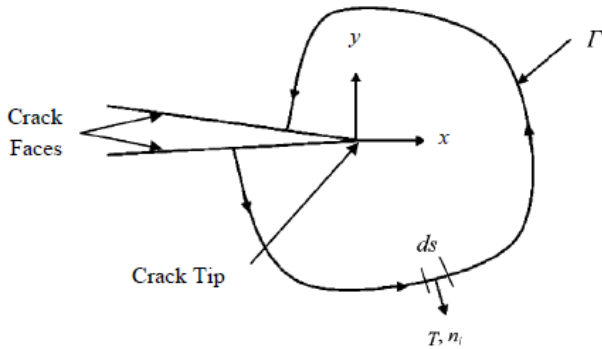


Figure 1. A definition of contour path to evaluate J-integral.

In ANSYS,  $J$ -integral is computed through the virtual crack extension (VCE) method or it is also called as domain integral method (Park [16]). In order to determine the  $J$ -integral, proper selection of contour path is important even though  $J$ -integral analysis is a path independent method. This is because large material shrinkage occurs around the crack tip (Rice [13]). In this work, 5<sup>th</sup> contour is selected which give 0.05% compared with 4<sup>st</sup> contour showing a path independent effect around the crack tip. All the calculations in determining the fracture parameters are conducted automatically through the use of ANSYS parametric design language (APDL).

### 3.0 Numerical Modelling

#### 3.1 Sickle-Shaped Surface Cracks

Due to the symmetrical effect only a quarter finite element model is used where the radius,  $R = 25\text{mm}$  and the half length of the solid round bar is  $200\text{mm}$ . Figure 2 shows the cross-sectional area of sickle-shaped surface crack where  $O$  and  $O'$  are the central point of circle and semi-ellipse, respectively. There are seven values of crack aspect or semi-elliptical ratios,  $a_{\text{minor}}/b_{\text{major}}$  are used ranging between 0.0 to 1.2 with an increment of 0.2. While, six relative crack depth,  $a/D$  are used namely 0.1, 0.2, 0.3, 0.4, 0.5 and 0.6. All of these are used in order to study the influence of different relative crack depths and crack aspect ratios on the stress intensity factors. The SIFs are determined at six different locations along the crack front and the SIF at the point  $C$  is not determined due to the singular problem. It is estimated that the nearest point close to point  $C$  is 83% measured from point  $A$ . The location of each point along the crack front is also normalized such as  $x/h$  for the location of point  $P$ .

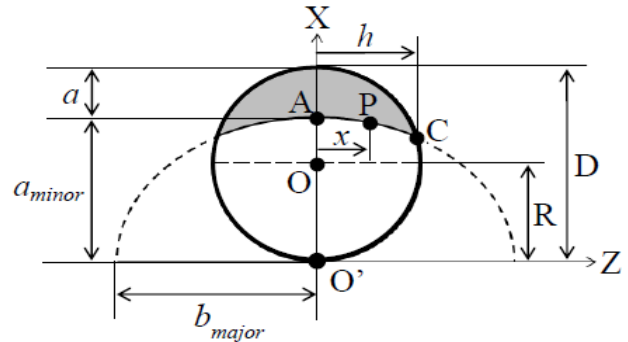


Figure 2. Nomenclature of sickle-shaped crack.

#### 3.2 Finite Element Modelling

The construction of finite element model is started with the model of cross-sectional area as shown in Figure 2. Once it is completed, the model is extruded along the  $y$ -axis with a length of  $200\text{mm}$ . The extruded volume model is presented in Figure 3(a). Special attention is given at the tip of the sickle-shaped crack where iso-parametric element SOLID186 is used. The square-root singularity of stresses and strains around the crack tip is modelled by shifting the mid-point nodes to the quarter-point location close to the tip. Firstly, the two-dimensional model is meshed and then it is swept along the crack front. Then, the remaining model is meshed with irregular similar element. The quarter finite element model is shown in Figure 3(b) with its corresponding crack tip singular element as in Figure 3(c).

The whole edge right surface is symmetrically constrained except the crack faces. The left surface plane is also symmetrically constrained as in Figure 4. There are two types of tension loading are used separately. The first tension pressure is directly applied onto the cross-sectional area of the left edge of the finite element model. This pressure is freed to move thus creating the effect of bending moment and it is called a free pressure,  $P_{fr}$ . Second type of tension pressure is allowed to move in  $y$ -

axis only and it is called a fix pressure,  $P_{fx}$ . The purpose of these forces is to compare the stress intensity factors and to study the SIF relationships when subjected to these forces.

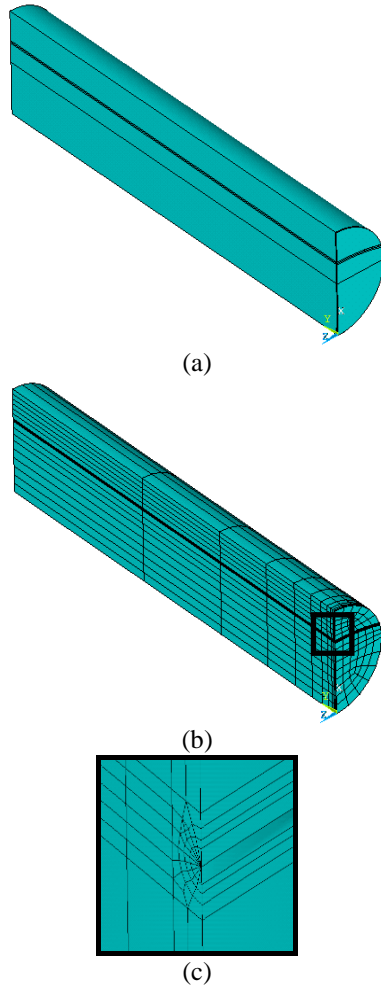


Figure 3. (a) An extruded volume cracked model, (b) Quarter finite element model and (c) Corresponding singular element around the crack tip.

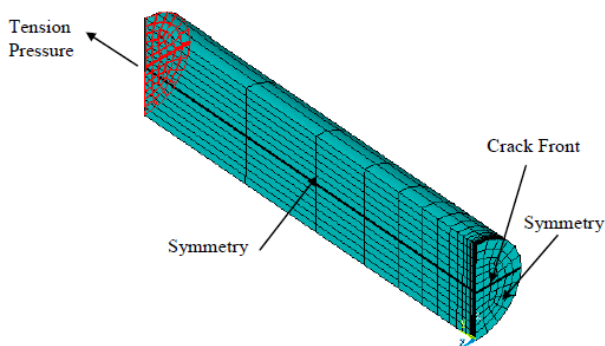


Figure 4. The boundary conditions and the loading on the finite element model.

The stress intensity factors (SIF) along the sickle-shape crack front are determined using ANSYS finite element program. The determination of SIFs is based on the J-integral where it can be directly converted into SIFs using Eq. (5) as long as the problem within the elastic ranges and has fulfilled the plain strain condition:

$$K_I = \sqrt{\frac{J_e E}{1-\nu^2}} \quad (5)$$

where,  $K_I$  is a mode I SIF,  $J_e$  is an elastic J-integral determined directly from the program,  $E$  is a modulus of elasticity and  $\nu$  is a Poisson's ratio. In order to generalize the SIFs, it is recommended to convert them into a normalized value called a mode I dimensionless SIF or geometrical correction factor,  $F_I$  as Eq. (6):

$$F_I = \frac{K_I}{\sigma \sqrt{\pi a}} \quad (6)$$

where,  $\sigma$  is a applied stress and  $a$  is a crack depth. In Eq. (6), there are two types of stresses which are the free stress,  $\sigma_{fr}$  and the fix stress,  $\sigma_{fx}$ . Then, consequently produced two types of SIFs as in Eqs. (7) and (8):

$$F_{I,fr} = \frac{K_{I,fr}}{\sigma_{fr} \sqrt{\pi a}} \quad (7)$$

$$F_{I,fx} = \frac{K_{I,fx}}{\sigma_{fx} \sqrt{\pi a}} \quad (8)$$

Before the model is further used, it is a compulsory to validate the present model is in the right condition. According to Figure 4, it is revealed that the present model is well agreed with the existing model. Therefore, this present model can be utilized for the further analysis.

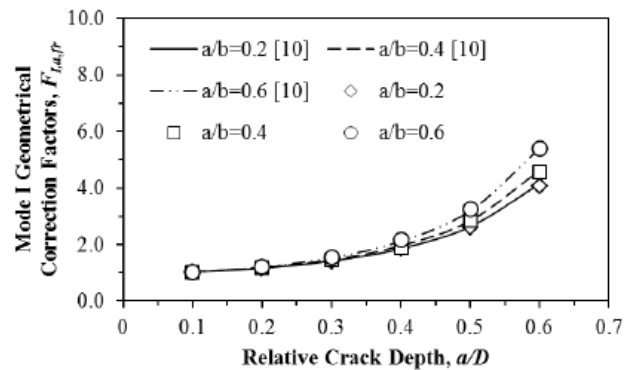


Figure 5. Model validations of the present and the existing models.

In order to study the role of bending effect when the free-type stress is used, both Eqs. (7) and (8) is then compared as in Eq. (9):

$$F_{I,fr} - F_{I,fx} = F^* \quad (9)$$

The purpose of this comparison is to obtain the SIFs due to the bending effect,  $F^*$  when it is subjected to free axial stress as reported in the first part of this paper [17]. For the sake of simplicity, only the SIFs at  $x/h = 0.0$  are considered with the assumption that the behavior of SIFs at other locations are similar.

## 4.0 Results and Discussion

### 4.1 Effect of Crack Aspect Ratios on the SIFs

The effect of crack geometries on the mode I SIFs are presented in Figure 6 when the values of  $a/b$  are varied and subjected to free-axial stress. The SIFs

obtained using fix-axial stresses are not presented since the behavior of these SIFs are similar but lower in magnitudes. For the relatively straight-fronted cracks ( $a/b \leq 0.2$ ), the SIFs along the crack fronts are almost flattened. However, the SIFs around the outer edge are slightly higher than the SIFs at the middle locations. This is due to when the crack is almost straight, the stresses are uniformly distributed along the crack front and therefore opening the crack faces in similar manner. When  $a/b > 0.4$ , different mechanisms are observed where the SIFs around the outer surface are decreased relative to the SIFs at the middle points. However, this behavior is only occurred for the case of deeper crack depth ( $a/D > 0.4$ ). The reductions of SIFs became significant when  $a/b$  increased. It is due to the fact that when  $a/b$  is increased, the shape of crack front changed from straight-fronted to the sickle-shaped cracks. When the cracks took the sickle shapes, the stress distributions are not uniform especially along the crack front where the crack can be classified according to position, the upper and side cracks. For the upper crack, it has experienced higher stress while the side crack is not. Then, the conditions of these crack contributed to the behavior of lower SIFs are occurred at the outer edge compared with the middle location.

#### 4.2 Effect of Relative Crack Depth on the SIFs

The effect of relative crack depth,  $a/D$  on the SIFs when the values of  $a/b$  are varies are depicted in Figure 7. It is revealed that similar distributions of SIFs are observed for all  $a/D$  cases excepted deeper the cracks higher the magnitudes of SIFs along the crack fronts. For the case of relatively shallow cracks ( $a/D \leq 0.3$ ),

#### 4.3 SIFs of Bending Moment Effects

Table 1 presents the SIFs at  $x/h = 0.0$  obtained using two types of axial stresses (free- and fix-stress condition). It is obvious that when free-axial stress is used, it is capable to induce the SIFs due to the bending effect. Whereas for fix-axial stress, it is only allowed to move in y-axial direction thus not creating the SIFs due to the bending effect. In order to examine such effect, Eq. (9) is used and the resultants SIFs between two types of stresses are listed in Table 2. On the other hand, Table 3 tabulates the SIFs subjected to bending moment for comparison purposes. It is revealed that for the condition of shallow cracks ( $a/D \leq 0.3$ ), the SIFs due to the bending effect are minimal when compared with the SIFs in Table 3 [17]. However, when deeper cracks are used ( $a/D > 0.3$ ), the SIFs are relatively similar with the SIFs under bending moment. Based on the observations from the previous works [9-12] most of the SIFs obtained using the free-axial stress but combined bending and tension stresses. Thus the SIFs in [9-12] have overestimated.

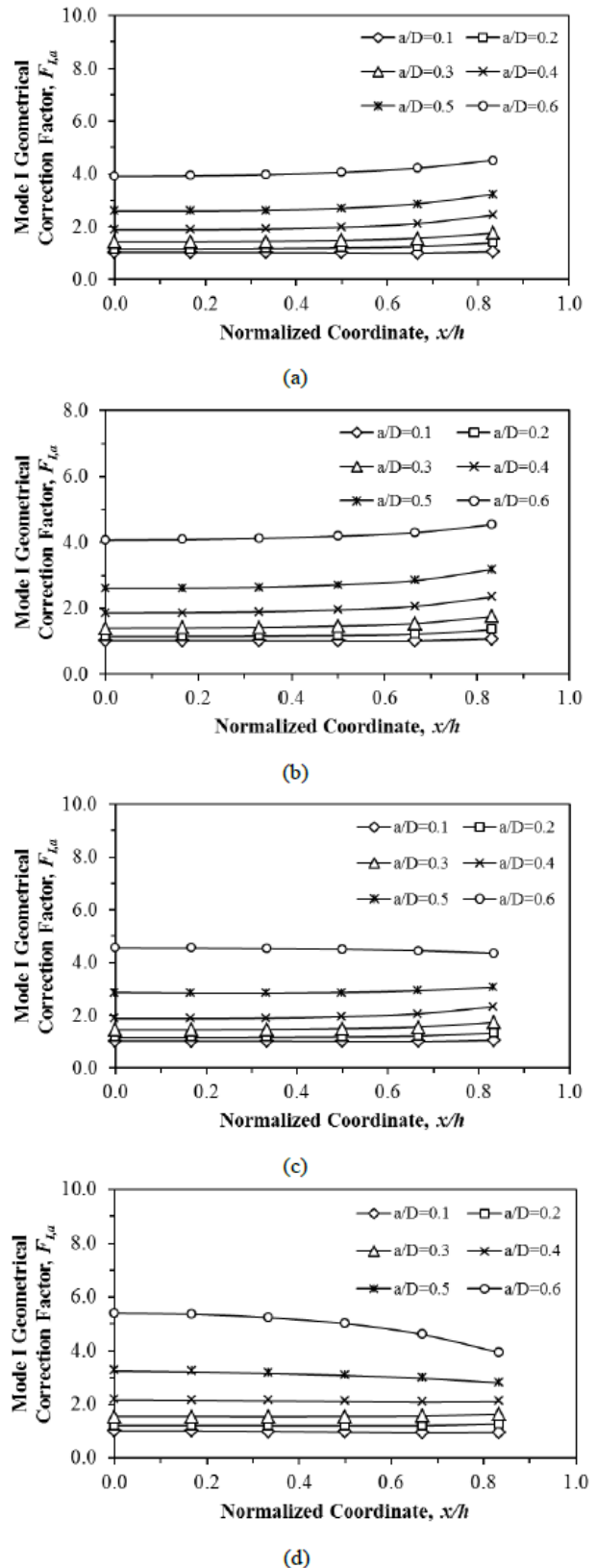


Figure 6. Continued.....

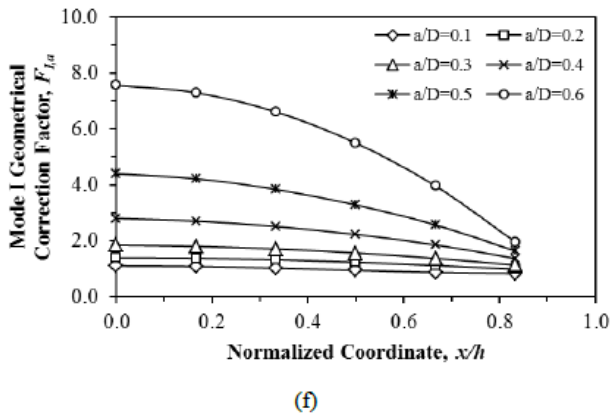


Figure 6. The effect of  $a/D$  on the mode I SIFs along the crack front for different  $a/b$ , (a) 0.0, (b) 0.2, (c) 0.4, (d) 0.6, (e) 0.8 and (f) 1.0.

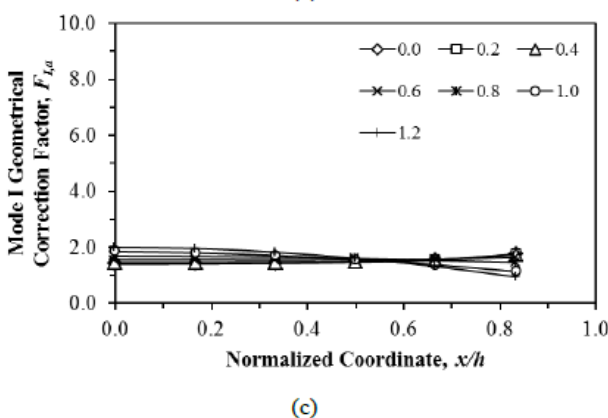
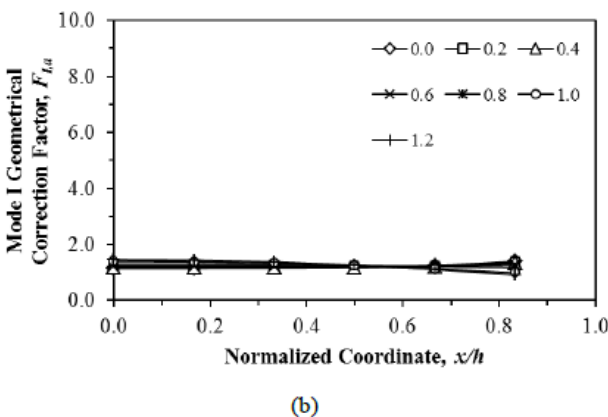
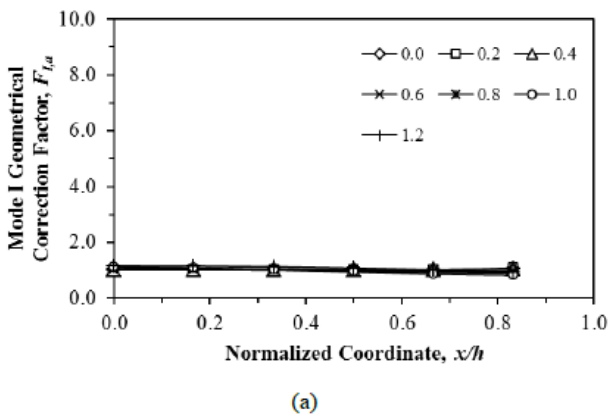
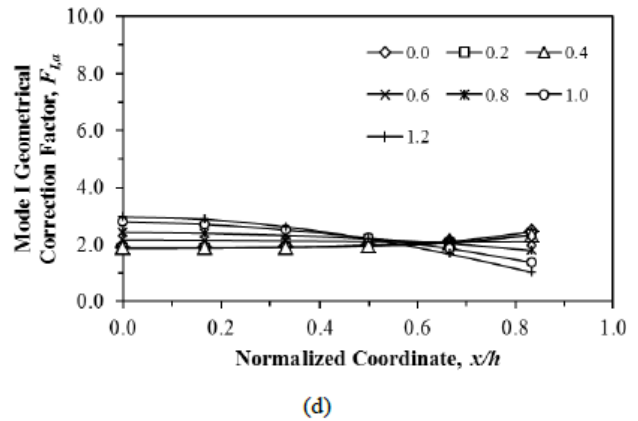


Figure 7. Continued.....

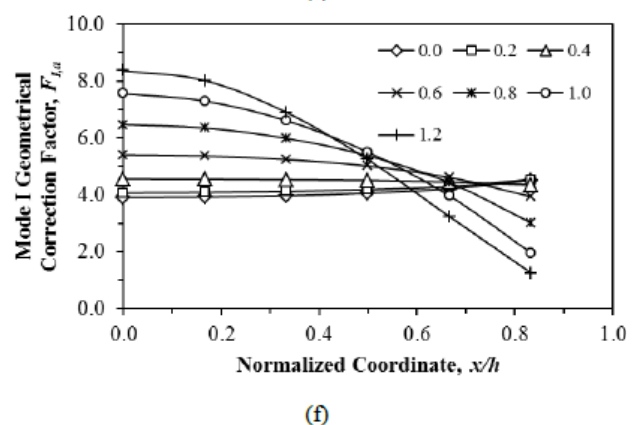
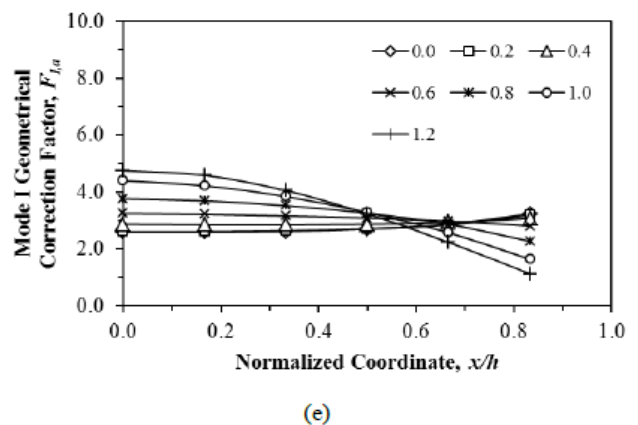


Figure 7. The effect of  $a/D$  on the mode I SIFs along the crack front for different  $a/b$ , (a) 0.1, (b) 0.2, (c) 0.3, (d) 0.4, (e) 0.5 and (f) 0.6.

#### 4.4 Sickle-Shaped Surface Crack Deformations

The effect of crack shapes strongly affected the distributions of SIFs along the crack front. Figure 8(a) reveals the deformations of crack faces for  $a/b = 0.0$  and  $a/D = 0.4$  under bending moment. For better visualization, all models are constructed in three-dimensional finite element model. For relatively straight crack ( $a/b \leq 0.2$ ), the crack has displaced almost uniformly across the crack front. This is suggested to conform that the SIFs along the crack front is almost flattened as shown in Figures 6(a). Referring to the yellow circle, the crack has opened uniformly without any closure effect. While Figure 8(b) shows the crack

deformation for  $a/b = 1.2$  and  $a/D = 0.4$ . There are two circles indicating two regions of opening and closing mechanisms. Red circle indicates that the crack experiences an opening mechanism. However, blue circle indicates that the region close to the outer point of the crack front has almost closed.

Table 1. SIFs at  $x/h = 0.0$  due to free-axial and fix-axial stresses.

$a/D$	$a/b$					
	0.0	0.2	0.4	0.6	0.8	1.0
SIFs under Free-Axial Stress, $F_{L,fr}$						
0.1	1.03	1.01	1.031	1.019	1.060	1.109
0.2	1.15	1.14	1.163	1.221	1.293	1.392
0.3	1.42	1.39	1.453	1.555	1.692	1.850
0.4	1.88	1.86	1.882	2.171	2.429	2.798
0.5	2.59	2.60	2.866	3.249	3.767	4.399
0.6	3.91	4.07	4.555	5.404	6.468	7.558
SIFs under Fix-Axial Stress, $F_{L,fx}$						
0.1	1.00	0.99	1.016	1.013	1.046	1.088
0.2	1.07	1.08	1.103	1.137	1.195	1.267
0.3	1.24	1.264	1.2993	1.3690	1.4707	1.6145
0.4	1.51	1.546	1.614	1.735	1.916	2.148
0.5	1.92	1.965	2.084	2.297	2.591	2.939
0.6	2.49	2.565	2.775	3.119	3.562	4.046

Table 2. SIFs due to Bending Effect at  $x/h = 0.0$ .

$a/D$	$a/b$					
	0.0	0.2	0.4	0.6	0.8	1.0
0.1	0.029	0.019	0.015	0.006	0.013	0.020
0.2	0.080	0.057	0.060	0.084	0.097	0.125
0.3	0.174	0.135	0.154	0.186	0.222	0.236
0.4	0.367	0.318	0.267	0.436	0.512	0.650
0.5	0.677	0.636	0.782	0.952	1.175	1.459
0.6	1.421	1.504	1.780	2.284	2.905	3.510

Table 3. SIFs under Bending Moment at  $x/h = 0.0$ ,  $F_{L,b}$  [17]

$a/D$	$a/b$					
	0.0	0.2	0.4	0.6	0.8	1.0
0.1	0.876	0.844	0.872	0.886	0.914	0.949
0.2	0.827	0.811	0.828	0.875	0.915	0.968
0.3	0.848	0.842	0.872	0.933	1.002	1.095
0.4	0.940	0.954	1.004	1.086	1.203	1.344
0.5	1.136	1.146	1.261	1.397	1.593	1.812
0.6	1.510	1.556	1.731	2.039	2.383	2.743

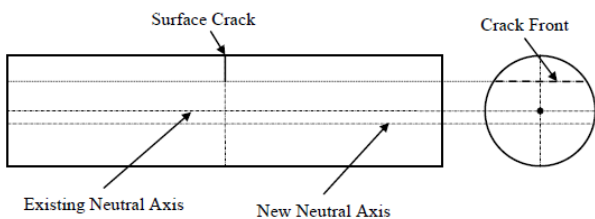


Figure 8. Effect of surface crack on the neutral axial of the solid round bar.

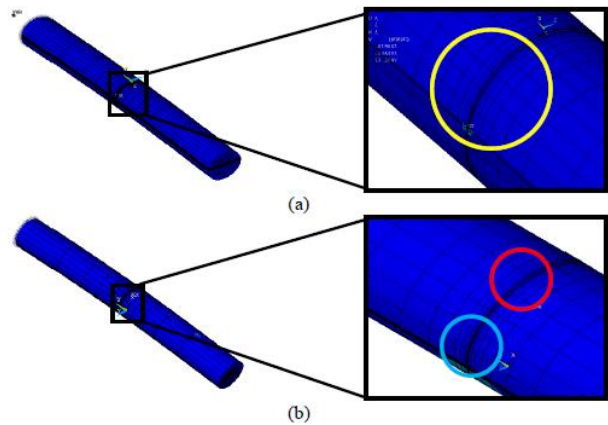


Figure 8. Crack deformations under free-axial tension stress, (a)  $a/b = 0.0$  and  $a/D = 0.4$  and (b)  $a/b = 1.2$  and  $a/D = 0.4$ .

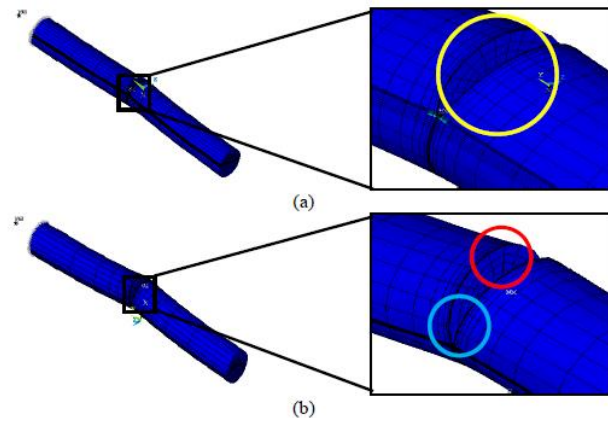


Figure 9. Crack deformations under fix-axial tension stress, (a)  $a/b = 0.0$  and  $a/D = 0.4$  and (b)  $a/b = 1.2$  and  $a/D = 0.4$ .

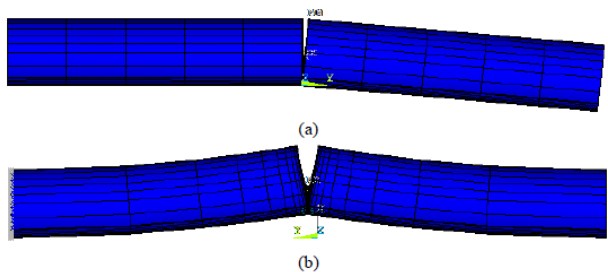


Figure 10. The deformations of solid round bars under (a) free-axial and (b) fix-axial stresses.

#### 4.4 Stress Intensity Factors at the $x/h = 0.0$

Figure 8 shows the variation of stress intensity factors (SIFs) at the middle point along the crack front ( $x/h = 0.0$ ) for different  $a/b$ . In general, higher SIFs are obtained when  $a/b$  ratios increased. For the relatively shallow cracks in this case  $a/D \leq 0.2$ , the effects of geometries on the SIFs are insignificant. However when deeper cracks are used, the role of  $a/b$  became paramount important. Figure 8 also reveals that when higher  $a/b$  is used, the maximum SIFs occurred at the middle point

along the crack front. It is indicated that under bending moment, the crack started to initiate firstly at the mid-point before going to other locations. For the case of  $a/b \leq 0.2$  (straight and almost straight-fronted cracks), the SIFs for  $a/D < 0.4$  are relatively flattened. This is to show that the cracks grew along the crack front are almost uniform where the tendency of the crack to initiate probably in a similar manner.

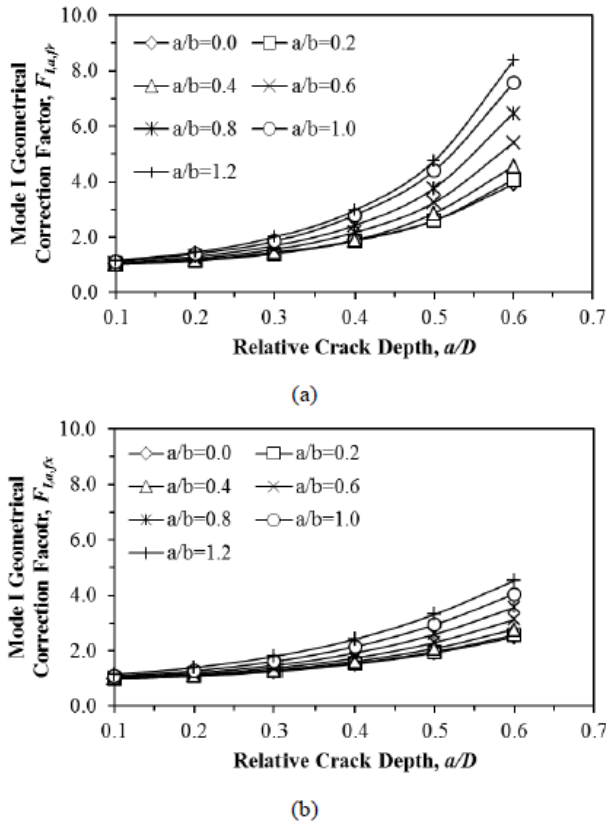


Figure 8. The SIFs for different  $a/b$  at the  $x/h = 0.0$ , (a) free- and (b) fix-stresses.

### 5.0 Summary

In this paper, the behavior of sickle-shaped surface cracks in round bars are investigated and analysis where it is subjected to tension force. The stress intensity factors (SIF) are based on the  $J$ -integral. Then the normalized SIFs are plotted against the normalized locations along the crack front. Seven crack aspect ratios,  $a/b$  and six relative crack depth,  $a/D$  are modeled using ANSYS finite element program. According to the numerical simulations, it is found that:

- i. For the shallow cracks ( $a/D \leq 0.3$ ), the SIFs have no significant different even though different  $a/b$  are used.
- ii. For straight or relatively straight cracks ( $a/b \leq 0.2$ ), the distributions of SIFs along the crack fronts are almost flattened. However when  $a/b > 0.2$  are used, the SIFs around the outer surfaces are relatively lower that the SIFs close to the central regions.

- iii. From numerical simulations, it is observed that the circumferential side cracks experiences insignificant mode I opening mechanisms compared with the crack located at the upper side.

### References

- [1] Nurdin A, Mustapa, MS, Ghazali MI, Sujitno T and Ridha M. 2013. Fatigue Life Prediction of Commercially Pure Titanium after Nitrogen Ion Implantation. *International Journal of Automotive and Mechanical Engineering*, Volume 7, pp. 1005-1013.
- [2] Daud R, Ariffin AK, and Abdullah S. 2013. Validation of Crack Interaction Limit Model for Parallel Edge Cracks Using Two-Dimensional Finite Element Analysis. *International Journal of Automotive and Mechanical Engineering*, Volume 7, pp. 993-1004.
- [3] Ismail AE, Ariffin AK, Abdullah S and Ghazali MJ. 2012. Off-set crack propagation analysis under mixed mode loadings. *International Journal of Automotive Technology*, Volume 12, Number 2, pp. 225-232.
- [4] Ismail AE, Ariffin AK, Abdullah S and Ghazali MJ. 2012. Stress intensity factors for surface cracks in round bar under single and combined loadings. *Meccanica*, Volume 47, Number 5, pp.1141-1156.
- [5] Toribio J, Alvarez N, Gonzalez B, Matos JC. 2009. A critical review of stress intensity factor solutions for surface cracks in round bars subjected to tension loading. *Engineering Failure Analysis*, 16:794-809.
- [6] Carpinteri A, Vantadori S. Sickle-shaped cracks in metallic round bars under cyclic eccentric axial loading. *International Journal of Fatigue*. 2009, Volume 31, pp. 759-765.
- [7] Mattheck C, Morawietz, Munz D. 1985. Stress intensity factors of sickle-shaped cracks in cylindrical bars. *International Journal of Fatigue*, Volume 7, Number 1, pp. 45-47.
- [8] Hobbs J, Burguete R, Heyes P, Patterson E. 2001. A photoelastic analysis of crescent-shaped cracks in bolts. *The Journal of Strain Analysis for Engineering Design*, Volume 36, Number 1, pp. 93-99.
- [9] Carpinteri A, Brighenti R, Vantadori S, Viappiani D. 2006. Sickle-shaped crack in a round bar under complex mode I loading. *Fatigue and Fracture of Engineering Materials and Structures*, Volume 30, pp. 524-534.
- [10] Carpinteri A, Vantadori S. 2009. Sickle-shaped surface crack in a notched round bar under cyclic tension and bending. *Fatigue and Fracture of Engineering Materials and Structures*, Volume 32, pp. 223-232.
- [11] Ismail AE, Ariffin AK, Abdullah S, Ghazali AJ. 2012. Stress intensity factors under combined tension and torsion loadings. *Indian Journal of Engineering and Materials Science*, Volume 19, pp. 5-16.
- [12] Ismail AE, Ariffin AK, Abdullah S, Ghazali AJ. 2012. Stress intensity factors under combined

bending and torsion moments. *Journal of Zhejiang University-Science A (Applied Physics and Engineering)*, Volume 13, Number 1, pp.1-8.

[13] Rice JR. 1968. A path independent integral and the approximate analysis of strain concentration by notches and cracks. *Journal of Applied Mechanics*, Volume 35, pp. 379-386.

[14] Kumar V, German MD, Shih, CF. 1981. An engineering approach for elastic-plastic fracture analysis. EPRI NP-1931, Project 1237.

[15] Rahman S. 2001. Probabilistic fracture mechanics: J-estimation and finite element methods. *Engineering Fracture Mechanics*, Volume 68, pp. 107-125.

[16] Parks DM. 1977. The virtual crack extension method for nonlinear material behavior. *Computer Methods in Applied Mechanics and Engineering*, Volume 12, pp. 353-364.

[17] A.E Ismail. Mode I stress intensity factor of sickle shaped cracks in round solid bars under bending moment. *International Journal of Automotive and Mechanical Engineering* (under review).

Table 2. SIFs of Sickle-Shaped Crack under Fix-Axial Tension Stress,  $F_{I,fx}$ .

$x/h$	$a/D$	$a/b$						
		0.0	0.2	0.4	0.6	0.8	1.0	1.2
0.00	0.1	1.0008	0.9999	1.0162	1.0138	1.0466	1.0888	1.1467
	0.2	1.0784	1.0872	1.1031	1.1373	1.1953	1.2671	1.3882
	0.3	1.2476	1.2642	1.2993	1.3690	1.4707	1.6145	1.7976
	0.4	1.5179	1.5463	1.6145	1.7354	1.9165	2.1486	2.4170
	0.5	1.9206	1.9650	2.0847	2.2971	2.5914	2.9395	3.3107
	0.6	2.4928	2.5658	2.7753	3.1194	3.5625	4.0463	4.5290
0.17	0.1	1.0079	1.0060	1.0219	1.0198	1.0503	1.0910	1.1405
	0.2	1.0860	1.0947	1.1097	1.1432	1.1975	1.2632	1.3715
	0.3	1.2556	1.2729	1.3063	1.3734	1.4697	1.6018	1.7642
	0.4	1.5284	1.5558	1.6216	1.7371	1.9080	2.1207	2.3572
	0.5	1.9318	1.9763	2.0896	2.2934	2.5701	2.8876	3.2111
	0.6	2.5029	2.5770	2.7768	3.1055	3.5208	3.9597	4.3766
0.33	0.1	1.0236	1.0226	1.0374	1.0318	1.0568	1.0922	1.1141
	0.2	1.1079	1.1155	1.1277	1.1553	1.1993	1.2459	1.3116
	0.3	1.2781	1.2969	1.3252	1.3822	1.4587	1.5531	1.6518
	0.4	1.5576	1.5822	1.6393	1.7367	1.8723	2.0227	2.1621
	0.5	1.9648	2.0065	2.1023	2.2729	2.4899	2.7087	2.8912
	0.6	2.5378	2.6059	2.7744	3.0469	3.3672	3.6610	3.8851
0.50	0.1	1.0561	1.0546	1.0647	1.0544	1.0704	1.0965	1.0710
	0.2	1.1495	1.1556	1.1620	1.1789	1.2019	1.2135	1.2129
	0.3	1.3212	1.3437	1.3620	1.3996	1.4389	1.4677	1.4710
	0.4	1.6141	1.6345	1.6738	1.7355	1.8070	1.8519	1.8563
	0.5	2.0279	2.0642	2.1246	2.2342	2.3441	2.4029	2.3992
	0.6	2.6036	2.6595	2.7686	2.9380	3.0908	3.1598	3.1426
0.67	0.1	1.1146	1.1104	1.1158	1.0966	1.0946	1.1051	1.0088
	0.2	1.2270	1.2314	1.2273	1.2247	1.2116	1.1610	1.0736
	0.3	1.4010	1.4318	1.4317	1.4332	1.4083	1.3365	1.2247
	0.4	1.7192	1.7304	1.7383	1.7360	1.7009	1.5967	1.4544
	0.5	2.1413	2.1675	2.1635	2.1671	2.1085	1.9586	1.7741
	0.6	2.7183	2.7521	2.7576	2.7529	2.6561	2.4507	2.2194
0.83	0.1	1.2313	1.2266	1.2212	1.1836	1.1500	1.1331	0.9301
	0.2	1.4005	1.3983	1.3730	1.3275	1.2459	1.0883	0.8832
	0.3	1.5801	1.6341	1.5930	1.5188	1.3692	1.1384	0.9011
	0.4	1.9565	1.9480	1.8854	1.7496	1.5228	1.2249	0.9618
	0.5	2.3806	2.3871	2.2310	2.0473	1.7264	1.3542	1.0494
	0.6	2.9334	2.9248	2.7266	2.4233	1.9844	1.5285	1.1833